Synthesis, Characterization, and Properties of Polyelectrolyte Block Copolymer Brushes Prepared by Atom Transfer Radical Polymerization and Their Use in the Synthesis of Metal Nanoparticles

Stephen G. Boyes,[‡] Bulent Akgun,[†] William J. Brittain,*[,†] and Mark D. Foster[†]

Department of Polymer Science, The University of Akron, Akron, Ohio 44325-3909, and School of Polymers and High Performance Materials, University of Southern Mississippi, Hattiesburg, Mississippi 39406-0076

Received July 18, 2003; Revised Manuscript Received October 8, 2003

ABSTRACT: Diblock copolymer polyelectrolyte brushes of either polystyrene (PS) or poly(methyl acrylate) (PMA) and poly(acrylic acid) (PAA) were synthesized using sequential monomer addition from a tethered 2-bromoisobutyrate initiator. Si/SiO_2//PS-*b*-poly(*tert*-butyl acrylate) (P(*t*-BA)) and Si/SiO_2//PMA-*b*-P(t-BA) were prepared by the "grafting from" method using atom transfer radical polymerization. The PAA block was prepared by hydrolysis of poly(*tert*-butyl acrylate) (P(*t*-BA)) and the polyelectrolyte was formed by subsequent treatment with either aqueous silver acetate or sodium tetrapalladate. Conversion of P(*t*-BA) to PAA and attachment of either silver or palladium ions to the PAA block was confirmed using ATR-FTIR spectroscopy, water contact angle measurements, and X-ray photoelectron spectroscopy. Solvent switching of the diblock copolymer brush using DMF and anisole was incomplete both before and after treatment with silver acetate, although the degree of switching was larger before treatment. The polyelectrolyte diblock copolymer brushes were used for the synthesis of inorganic nanoparticles by reduction of the treated PAA. These samples were characterized using AFM, XPS, and ATR−FTIR.

Introduction

Polymer brushes refer to an assembly of polymer chains which are tethered by one end to a surface or interface.[1,2] Tethering of the chains in close proximity to each other forces the chains to stretch away from the surface to avoid overlapping. Polymer brushes have recently attracted considerable attention, and there have been numerous studies to examine their structure and novel properties.[3−9] Polymer brushes are typically synthesized by two different methods: physisorption and covalent attachment. Of these methods, covalent attachment is preferred as it overcomes the disadvantages of physisorption which include thermal and solvolytic instabilities.[10] Covalent attachment of polymer brushes can be achieved by either "grafting to" or "grafting from" techniques. The "grafting to" technique involves tethering preformed end-functionalized polymer chains to a suitable substrate under appropriate conditions,[11] whereas the "grafting from" technique involves the immobilizing of initiators onto the substrate followed by in situ surface-initiated polymerization to generate the tethered polymer brush. The "grafting from" approach has generally become the most attractive way to prepare thick, covalently tethered polymer brushes with a high grafting density.[10]

Recent advances in polymer synthesis techniques have given rise to the importance of controlled/living free radical polymerization, as it provides a number of advantages over traditional free radical techniques.[12] The main advantages that a controlled/living free radical system provides for polymer brush synthesis are control over the brush thickness, via control of molecular weight and narrow polydispersities, and the ability to prepare block copolymers by the sequential activation of the dormant chain end in the presence of different monomers.[13,14] Probably the most common "living" radical technique to produce polymer brushes is atom transfer radical polymerization (ATRP).[15−20] Recently, the use of ATRP to produce tethered polyelectrolyte brushes has been reported.[21] Surfaces functionalized with polyelectrolyte brushes have stimulated significant theoretical[22−24] but limited experimental[21,25,26] interest. Such surfaces may have important applications in fields such as "smart" coatings, biosensors, and colloid stabilization. Another potential use for polyelectrolyte brushes is in the synthesis of inorganic nanoparticles.

The synthesis of inorganic nanoparticles in a polyelectrolyte matrix has been previously documented.[27−29] Nanometer-sized inorganic particles potentially have unique properties due to quantum confinement effects and their large surface area relative to their volume.[29] Wang and co-workers[29] demonstrated the in situ preparation of inorganic nanoparticles in polyelectrolyte multilayer films. The multilayer films were formed by the layer-by-layer adsorption of oppositely charged weak polyelectrolytes. One of the weak polyelectrolytes used to synthesize the multilayer was poly(acrylic acid) (PAA). The use of PAA allows the binding of metal cations, from aqueous solution, to the carboxylic acid groups. The bound cations can then be subsequently reduced to produce inorganic nanoparticles trapped within the film.

The use of "living" radical polymerization techniques to produce diblock copolymer brushes of polystyrene (PS) and PAA has been previously reported.[16] However, to date there has been no report on the use of diblock copolymer brushes, containing a PAA block, to synthesize polyelectrolyte diblock copolymer brushes and subsequently inorganic nanoparticles. In this report we detail the use of ATRP to synthesize polyelectrolyte brushes of either styrene or methyl acrylate and poly(acrylic acid) modified by treatment with an aqueous

[†] The University of Akron.
[‡] University of Southern Mississippi.

10.1021/ma035029c CCC: $25.00 © 2003 American Chemical Society
Published on Web 11/20/2003

solution of metal cations. Nanoparticles of silver and palladium were synthesized by reduction of the polyelectrolyte diblock copolymer brushes, and the resultant systems were characterized using FTIR, tensiometry, ellipsometry, atomic force microscopy (AFM), and X-ray photoelectron spectroscopy (XPS).

Experimental Section

Materials. Styrene (S, Aldrich, 99%), methyl acrylate (MA, Aldrich, 99%), and *tert*-butyl acrylate (*t*-BA, Aldrich, 98%) were passed through a column of activated basic alumina and degassed with high-purity nitrogen for 1 h prior to use. CuBr (Aldrich, 98%) was purified as described in the literature.[30] *N*,*N*,*N*′,*N*′,*N*″-Pentamethyldiethylenetriamine (PMDETA, Aldrich, 99%), ethyl 2-bromoisobutyrate (Br-iB, Aldrich, 98%), silver acetate (Ag(Ac), Aldrich, 99.999%), sodium tetrachloropalladate(II) (Na_2PdCl_4, Aldrich, 98%), anhydrous anisole (Aldrich), and anhydrous acetone (Aldrich, HPLC grade) were used as received. Silicon ATR crystals (25 × 5 × 1 mm) were obtained from Harrick Scientific. Silicon wafers were purchased from Polishing Corporation of America. All other reagents were purchased from either Aldrich or Fisher Scientific and used as received.

Substrate Preparation. ATR crystals and silicon wafers were cleaned by treatment with freshly prepared "piranha" solution (70/30, v/v, concentrated H_2SO_4/30% aqueous H_2O_2) at 100 °C for 2 h and were then rinsed with distilled water and dried with a stream of clean air. It should be noted that the "piranha" solution is extremely reactive and should be handled with the appropriate care.

General Procedure for Deposition of Surface Bound Initiator. Into a dried round-bottom flask was placed a freshly cleaned silicon wafer and ATR crystal. The flask was sealed using a septum and flushed with high-purity nitrogen for 30 min. Dry toluene (10 mL) and a 25 vol % solution of the trichlorosilane initiator in toluene (0.2 mL) were added to the flask via syringe, and the flask was heated at 60 °C for 4 h under an atmosphere of nitrogen. The silicon wafer and ATR crystal were then removed, sequentially washed with toluene and ethanol, and then dried in a stream of air.

Typical Procedure for Surface ATRP from a Flat Silicon Substrate. An ATR crystal and silicon wafer were placed in a 100 mL Schlenk flask and sealed with a rubber septum. The flask was evacuated and back-filled with nitrogen three times and left under a nitrogen atmosphere. CuBr, solvent, and monomer were added to a separate 100 mL Schlenk flask with a magnetic stirrer bar, sealed with a rubber septum, and degassed by purging with nitrogen for 1 h. PMDETA was added to the mixture via a syringe, and the solution was stirred at reaction temperature until it became homogeneous (approximately 5 min). The solution was then transferred to the flask containing the ATR crystal and silicon wafer via cannula, followed by the addition of free initiator (Br-iB) via a syringe. The final concentrations were as follows: $[S]_0 = 3.9$ M, $[PMDETA]_0 = 25$ mM, $[CuBr]_0 = 12$ mM and $[Br\text{-}iB]_0 = 10$ mM or $[MA]_0 = 3.7$ M, $[PMDETA]_0 = 25$ mM, $[CuBr]_0 = 12$ mM and $[Br\text{-}iB]_0 = 10$ mM. The solvent used for the styrene and methyl acrylate polymerizations was anisole. The polymerization was allowed to proceed at reaction temperature for a specified time, after which the ATR crystal and silicon wafer were removed and rinsed with THF. To remove untethered polymer, the ATR crystal and silicon wafer were placed in a Soxhlet extractor and extracted with THF for 24 h, after which they were removed and sonicated in THF for 30 min. Free polymer from the polymerization solution was isolated by first evaporating residual monomer and solvent, dissolving in THF, and then passing the THF/polymer solution through a short column of activated basic alumina to remove any residual catalyst.

Block Copolymerizations. Block copolymerizations were performed in the same manner as the typical ATRP procedures for styrene or MA. The order of addition was governed by the use of ATR crystals and silicon wafers containing the initial polymer brushes. For example, the Si/SiO_2//PS-*b*-P(*t*-BA) brush was produced by performing the following typical ATRP procedures in order: styrene and *tert*-butyl acrylate. The final concentrations for the *t*-BA polymerizations were $[t\text{-}BA]_0 = 4.6$ M, $[PMDETA]_0 = 15$ mM, $[CuBr]_0 = 15$ mM, and $[Br\text{-}iB]_0 = 20$ mM. Anhydrous acetone was used as the solvent for the *t*-BA polymerizations. After each polymerization the ATR crystal and silicon wafer were cleaned and extracted to remove any untethered polymer before proceeding to the next polymerization.

Hydrolysis of Poly(*tert*-butyl acrylate) Block to Poly(acrylic acid) (PAA). The silicon wafer and ATR crystal containing the tethered diblock copolymer brush, with a P(*t*-BA) block, were placed in a 50 mL round-bottom flask. 30 mL of 10% aqueous HCl was added, and the flask was heated to reflux overnight, after which the wafer and crystal were removed, rinsed with water and ethanol, and then dried in a stream of air.

Reaction of PAA Block with Aqueous Metal Salts. The silicon wafer and ATR crystal containing the hydrolyzed polymer brush were placed in a vial containing 20 mL of a 10 mM aqueous solution of either silver acetate or sodium tetrachloropalladate. The vial was then covered completely with foil and heated at 40 °C for 24 h. After reaction, the wafer and crystal were removed, rinsed with distilled water, and then dried in a stream of air.

Treatment of Polyelectrolyte Brushes with Selective Solvents. The diblock copolymer sample was first immersed in good solvent for both blocks at 40 °C for 30 min to recover the original state. The sample was then immersed in a solvent, which was a good solvent for the block tethered to the wafer, but a poor or nonsolvent for the outer block, at 40 °C for 30 min. The sample was then removed from the solvent and dried with a stream of clean air followed by characterization with tensiometry, XPS, and AFM. This procedure was conducted on all diblock samples. DMF was used as a good solvent for PS, PMA, and PAA. Anisole was used as a good solvent for PS and PMA but a nonsolvent for PAA.

Reduction of Metal Ions Attached to Polyelectrolyte Brushes. The silicon wafer and ATR crystal containing the polymer brush that had been treated with the aqueous metal salt solutions were placed in a 100 mL Schlenk flask and sealed with a septum. The flask was then evacuated and backfilled with hydrogen at a pressure of 2 atm. The flask was then heated at 120 °C for 2 days, after which the wafer and ATR crystal were removed and characterized.

Characterization Methods. FTIR-ATR spectra were recorded using a Nicolet System 730 spectrometer using a modified 4XF beam condenser (Harrick Scientific). Spectra were recorded at 2 cm^{-1} resolution, and 500 scans were collected. Contact angles were determined using a Rame Hart NRL-100 contact angle goniometer equipped with an environmental chamber and tilting base mounted on a vibrationless table (Newport Corp.). Advancing and receding values were determined using the tilting stage method. Drop volumes were 10 μL. Ellipsometric measurements were performed on a Gaertner model L116C ellipsometer with He−Ne laser (λ = 632.8 nm) and a fixed angle of incidence of 70°. For the calculation of the layer thickness, refractive indices of n = 1.455 (for silicon oxide),[27] $n = 1.508$ (for the initiator layer), n = 1.5894 (for PS),[27] $n = 1.480$ (for PMA),[27] $n = 1.466$ (for P(*t*-BA)),[27] and $n = 1.527$ (for PAA)[27] were used. AFM was performed using a multimode scanning probe microscope (Park Scientific Autoprobe CP) in intermittent-contact mode with a silicon tip. The AFM images were obtained at room temperature in air. X-ray photoelectron spectroscopy (XPS) was performed on a Perkin-Elmer instrument using Al Kα radiation at The MATNET Surface Analysis Centre at Case Western Reserve University. The takeoff angle was 45°, and the incidence angle of X-rays was 45° with respect to surface normal, making the X-ray to electron angle 90°.

Results and Discussion

Synthesis and Characterization of Tethered Polyelectrolyte Brushes on Flat Silicate Sub-

Scheme 1. Synthesis of Si/SiO_2//PS-*b*-PAA(Ag^+) Brush on a Silicon Substrate

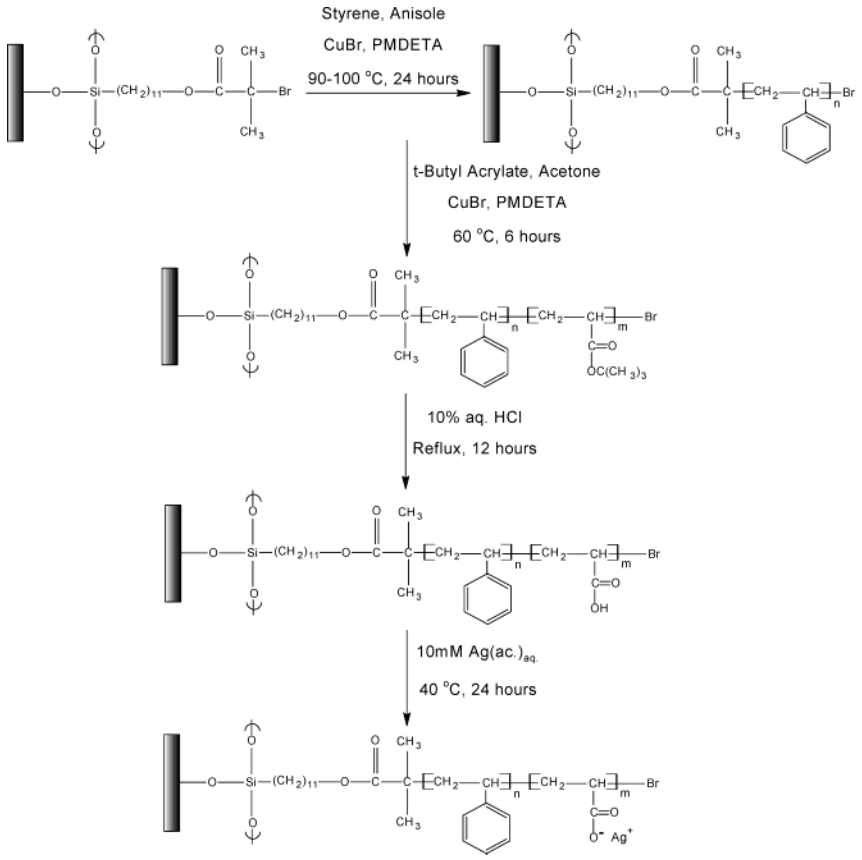

strates. The synthesis of tethered polyelectrolyte brushes of styrene or methyl acrylate and acrylic acid on flat silicate substrates via a "grafting from" approach is illustrated in Scheme 1. Scheme 1 outlines the preparation of Si/SiO_2//PS-*b*-PAA(Ag^+) diblock copolymer brush. A similar approach was used to synthesize a Si/SiO_2//PMA-*b*-PAA(Ag^+) and Si/SiO_2//PS-*b*-PAA(Pd^{2+}) diblock copolymer brushes. Preparation of the polyelectrolyte brushes involves immobilization of a bromoisobutyrate initiator onto a silicon substrate by self-assembly techniques followed by sequential ATRP of either styrene or methyl acrylate and *tert*-butyl acrylate to produce the desired diblock copolymer brush. The diblock copolymer brush, containing a *tert*-butyl acrylate block, was then hydrolyzed to the acrylic acid by refluxing the brush in a solution of 10% aqueous HCl for 12 h in the case of the Si/SiO_2//PS-*b*-P(*t*-BA) brush or 1 h in the case of the Si/SiO_2//PMA-*b*-P(*t*-BA) brush. The shorter refluxing time was used for the Si/SiO_2//PMA-*b*-P(*t*-BA) brush as longer refluxing resulted in degrafting of the polymer chains from the surface. After hydrolysis, both the Si/SiO_2//PS-*b*-PAA brush and the Si/SiO_2//PMA-*b*-PAA brush were treated with 10 mM aqueous silver acetate to form the polyelectrolyte diblock copolymer brush. An alternative polyelectrolyte diblock copolymer brush was formed by the treatment of a Si/SiO_2//PS-*b*-PAA brush with 10 mM aqueous sodium tetrachloropalladate.

The detailed experimental conditions for the ATRP reactions to produce the tethered polyelectrolyte diblock copolymer brush are described in the Experimental Section. The catalyst system used was CuBr/PMDETA, and in each case free initiator, ethyl 2-bromoisobutyrate, was added to the polymerization. It has been previously reported that free initiator is required to provide a sufficiently high concentration of deactivator, which is necessary for controlled polymerizations from the surface.[15] Table 1 outlines the properties for each of the layers of the diblock copolymer brushes produced. Each of the values shown is representative of the outer layer only. Molecular weight and polydispersity results for the tethered polymer chains are unavailable due to the fact that the diblock copolymer brushes were synthesized on low surface area substrates only. As such, degrafting of the tethered polymer chains would not produce enough sample for SEC analysis. The results in Table 1 indicate that after hydrolysis of the Si/SiO_2//PS-*b*-P(*t*-BA) brush, which has a 21 nm layer of styrene and a 17 nm layer of *t*-BA, there is a decrease in the thickness of the outer block from 17 to 8 nm and a dramatic decrease in the water contact angle of the surface, from

Table 1. Physical Properties of Polyelectrolyte Diblock Copolymer Brushes

brush structure	water contact angle[a] (deg) θ_a	θ_b	thickness[b] (nm)
Si/SiO_2//PS	99	84	21
Si/SiO_2//PS-*b*-P(*t*-BA)	95	84	17
Si/SiO_2//PS-*b*-PAA	complete wetting		8
Si/SiO_2//PS-*b*-PAA(Ag^+)	35	18	11
Si/SiO_2//PS	100	86	21
Si/SiO_2//PS-*b*-P(*t*-BA)	94	76	12
Si/SiO_2//PS-*b*-PAA	complete wetting		5
Si/SiO_2//PS-*b*-PAA(Pd^{2+})	26	9	11
Si/SiO_2//PMA	81	70	14
Si/SiO_2//PMA-*b*-P(*t*-BA)	95	82	16
Si/SiO_2//PMA-*b*-PAA	30	14	9
Si/SiO_2//PS-*b*-PAA(Ag^+)	40	25	13

[a] The standard deviation of contact angles was <2°. [b] Thickness determined by ellipsometry and is representative of the outer block only. Typical error on thickness measurement is ±1 nm.

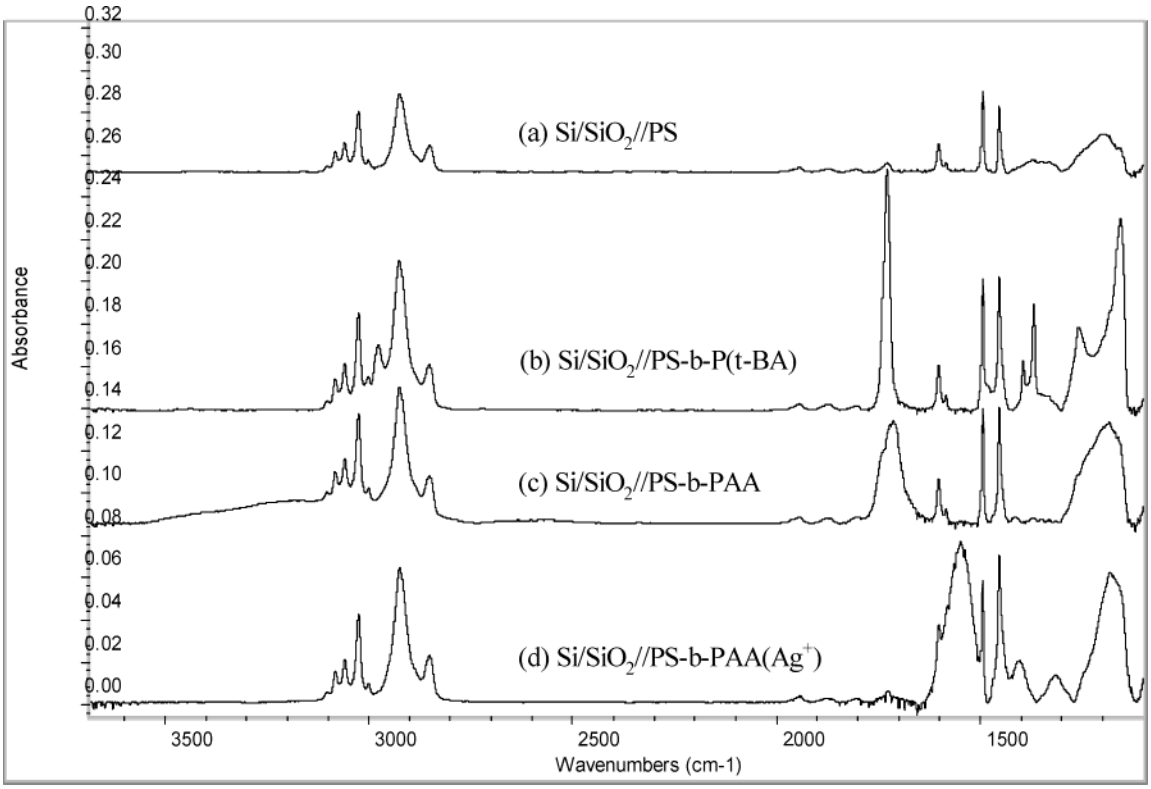

Figure 1. ATR−FTIR spectra of (a) Si/SiO_2//PS, (b) Si/SiO_2//PS-*b*-P(*t*-BA), (c) Si/SiO_2//PS-*b*-PAA, and (d) Si/SiO_2//PS-*b*-PAA-(Ag^+).

an advancing contact angle of 95° to a surface that is completely wettable. The decrease in thickness after hydrolysis is believed to be as a result of chain relaxation caused by removal of the bulky *tert*-butyl groups and has been reported by other research groups.[16] The dramatic decrease in advancing contact angle is believed to be due to the formation of the acrylic acid, as water is a good solvent for PAA and therefore should produce a surface which is completely wettable. Treatment of the Si/SiO_2//PS-*b*-PAA brush with aqueous silver acetate results in a slight increase in the thickness of the outer layer, from 8 to 11 nm, and a change in the contact angle from a completely wettable surface to an advancing contact angle of 35°. The increases in both the outer block thickness and advancing contact angle were attributed to the attachment of the silver ions to the PAA block. Similar results were seen for the formation of the Si/SiO_2//PS-*b*-PAA(Pd^{2+}) brush (Table 1). In this case, after hydrolysis the thickness of the P(*t*-BA) decreased from 12 to 5 nm, with the accompanying decrease in the advancing water contact angle from 94° to a completely wettable surface, indicating the formation of PAA. Treatment of this sample with aqueous sodium tetrachloropalladate resulted in a dramatic increase in the thickness of the outer block from 5 to 11 nm and produced a surface with an advancing contact angle of 26°. Again, these increases were attributed to attachment of the palladium ions to the PAA block.

The results for the Si/SiO_2//PMA-*b*-PAA(Ag^+) polyelectrolyte brush were slightly different than for the cases where PS was the tethered block adjacent to the surface. Hydrolysis of the Si/SiO_2//PMA-*b*-P(*t*-BA) brush, to produce the Si/SiO_2//PMA-*b*-PAA brush, resulted in a decrease of the thickness of the outer block from 16 to 9 nm but did not result in the surface being completely wettable. This is believed to be due to incomplete hydrolysis of the P(*t*-BA) block. As mentioned previously, the hydrolysis time for the Si/SiO_2//PMA-*b*-P(*t*-BA) brush was substantially less than the Si/SiO_2//PS-*b*-P(*t*-BA) brush, as long hydrolysis times resulted in degrafting of the polymer chains from the surface. This was presumably due to attack of the ester bond present in the initiator by the HCl, with this ester bond potentially being more accessible in the Si/SiO_2//PMA-*b*-P(*t*-BA) brush when compared to the Si/SiO_2//PS-*b*-P(*t*-BA) brush. However, after treatment of the Si/SiO_2//PMA-*b*-PAA brush with aqueous silver acetate, the thickness of the outer layer increased, from 9 to 13 nm, and the advancing contact angle increased, from 30° to 40°, again suggesting the attachment of silver ions.

The ATR−FTIR spectra for the synthesis of the tethered Si/SiO_2//PS-*b*-PAA(Ag^+) polymer brush are shown in Figure 1. The initial PS layer (Figure 1a) showed the characteristic peaks at 3026, 3060, and 3084 cm^{-1}, due to aromatic C−H stretching vibrations, and at 1453 and 1493 cm^{-1}, attributed to the aromatic C−C stretching vibrations. There are also both symmetric and asymmetric stretching vibrations due to the backbone CH_2 groups at 2850 and 2925 cm^{-1}, respectively. After reaction of the initial PS layer with *t*-BA, the ATR−FTIR spectra (Figure 1b) showed the presence of a peak at 1733 cm^{-1} due to the C═O stretch, a peak at 2976 cm^{-1} due to the asymmetric CH_3 stretching vibration, and a doublet at 1367/1392 cm^{-1} from the symmetric methyl deformation mode. Hydrolysis of the Si/SiO_2//PS-*b*-P(*t*-BA) brush to produce the Si/SiO_2//PS-*b*-PAA brush was confirmed by ATR−FTIR (Figure 1c), which showed the presence of a broad OH stretch at 2900−3400 cm^{-1}, a broadening and slight downward shift of the C═O peak to 1710 cm^{-1}, and loss of both the asymmetric CH_3 stretch and symmetric methyl

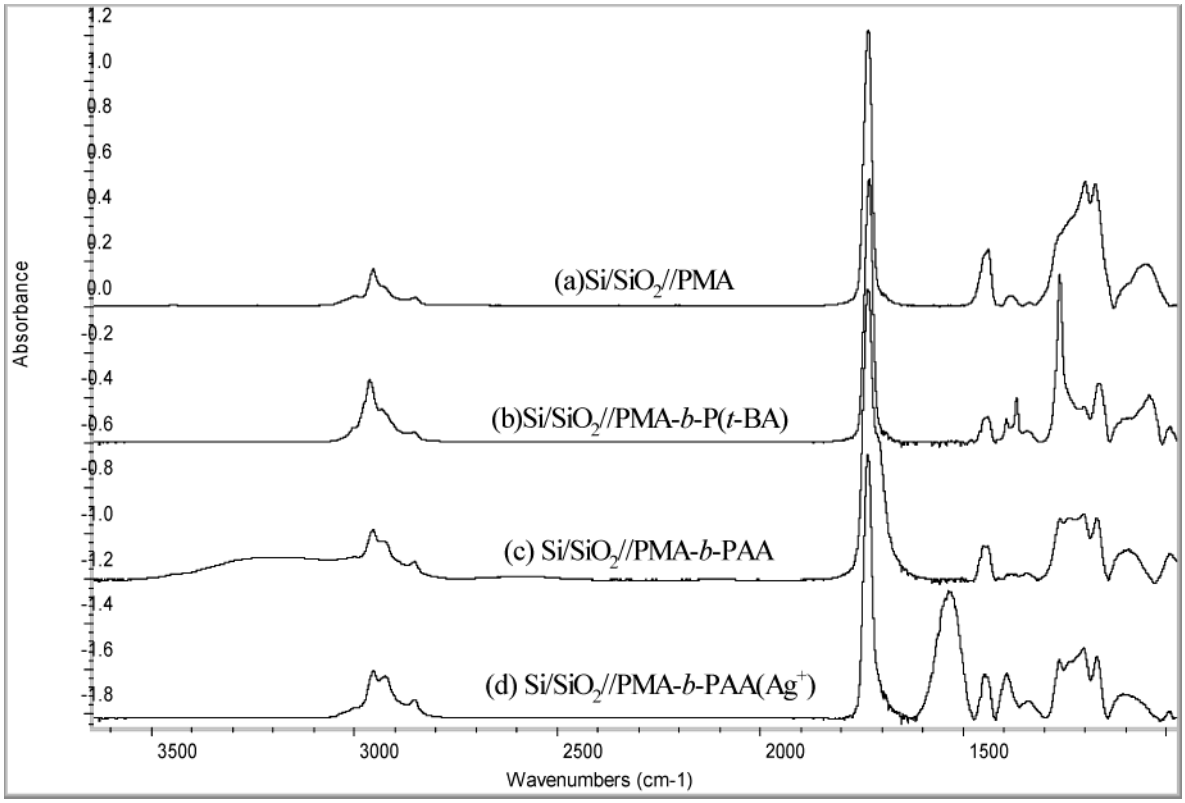

Figure 2. ATR−FTIR spectra of (a) Si/SiO_2//PMA, (b) Si/SiO_2//PMA-*b*-P(*t*-BA), (c) Si/SiO_2//PMA-*b*-PAA, and (d) Si/SiO_2//PMA-*b*-PAA(Ag^+).

deformation doublet due to removal of the *tert*-butyl group. Treatment of Si/SiO_2//PS-*b*-PAA brush with aqueous silver acetate resulted in loss of the broad OH peak and a shift in the C═O peak at 1710 cm^{-1} to 1548 cm^{-1} which was attributed to the formation of the carboxylate anion. Similar results were seen in the ATR−FTIR spectra for the synthesis of the Si/SiO_2//PS-*b*-PAA(Pd^{2+}) brush.

The ATR−FTIR spectra for the synthesis of the tethered Si/SiO_2//PMA-*b*-PAA(Ag^+) brush are shown in Figure 2. The spectra of the PMA block (Figure 2a) showed characteristic peaks at 2924 and 2852 cm^{-1} for asymmetric CH_2 stretching and symmetric CH_2 stretching, respectively, and also at 1734 cm^{-1} for the C═O stretch. Addition of a P(*t*-BA) block is identified (Figure 2b) by the presence of the symmetric methyl deformation doublet at 1365/1390 cm^{-1}. As with the previous sample, hydrolysis of the P(*t*-BA) block to produce PAA results in a broad OH peak, a broad shoulder on the carbonyl peak, and loss of the peaks associated with the *tert*-butyl group (Figure 2c). Upon treatment of the Si/SiO_2//PMA-*b*-PAA brush with aqueous sodium tetrachloropalladate, a peak appears at 1549 cm^{-1} due to the formation of the carboxylate anion, and the broad OH peak disappears (Figure 2d).

To further confirm the attachment of the metal cations to the PAA blocks of the diblock copolymer brushes, XPS was used to examine the surface both before and after treatment with the aqueous solutions of the metal salts. The sampling depth of the XPS experiments is approximately 5−10 nm, depending on the core level binding energy and takeoff angle.[31] Figure 3 shows the XPS spectra of a Si/SiO_2//PS-*b*-PAA diblock copolymer brush before treatment with aqueous silver acetate (Figure 3a) and after treatment with aqueous silver acetate for 24 h at 40 °C (Figure 3b). The main peaks on the XPS spectra of the sample before treatment are due to carbon, 72.8%, and oxygen, 22.3%. Other peaks present in the spectra are due to silicon (3.9%), nitrogen (0.7%), and fluorine (0.2%). After treatment of the Si/SiO_2//PS-*b*-PAA brush with aqueous silver acetate, the XPS spectra (Figure 3b) show the presence of a large amount of silver on the surface (9.6%). As the sample is rinsed repeatedly with distilled water after treatment with aqueous silver acetate, and the IR spectra of this sample (Figure 2d) show the presence of a peak due to the carboxylate anion, we conclude that this silver is attached to the PAA block of the brush and has thus formed a polyelectrolyte diblock copolymer brush. The XPS spectra after treatment has carbon (64.5%) and oxygen (23.5%) values similar to the values before treatment and also shows the presence of chlorine (1.7%), calcium (0.5%), and sodium (0.2%).

From the oxygen content of the Si/SiO_2//PS-*b*-PAA-(Ag^+) brush we are able to estimate the degree of loading of metal cations on the PAA block. To do this, we assume the value for the oxygen content is a result of the oxygen in the PAA block only and that the cations bind only to the ionized oxygen in the PAA block. Using these assumptions, the loading of cations on to the PAA block is calculated to be 88%. This indicates that the vast majority of the segments in the PAA block have cations attached. The term metal cations is used instead of simply silver ions as there is a small percentage of calcium and sodium also detected in the Si/SiO_2//PS-*b*-PAA(Ag^+) brush, and we assume that these cations are also bound to the PAA block. Similar results were seen for the XPS spectra of the Si/SiO_2//PMA-*b*-PAA brush both before and after treatment with aqueous silver acetate. In this case we are unable to calculate the loading of cations onto the PAA block as some of the

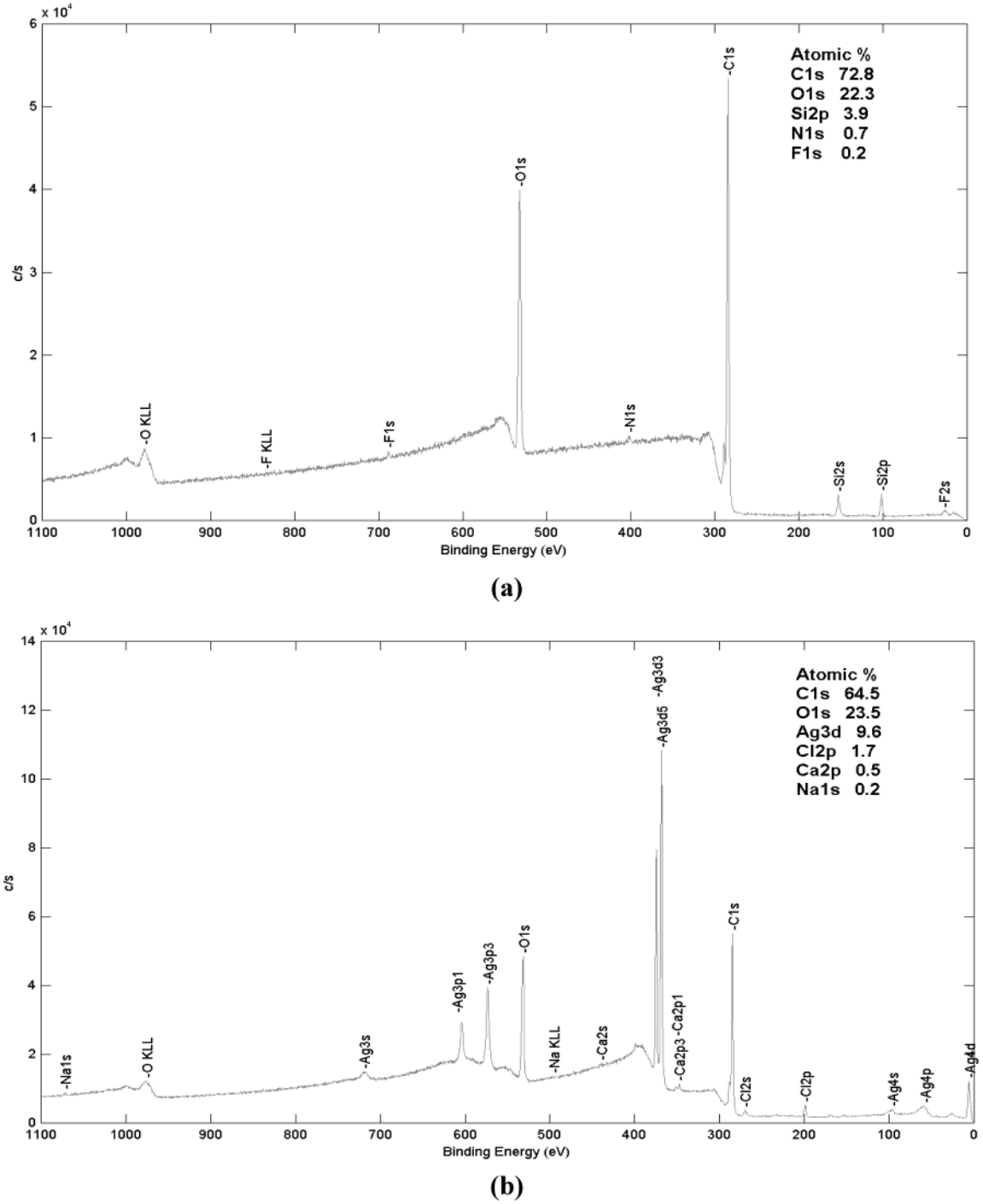

Figure 3. XPS spectra of the Si/SiO_2//PS-*b*-PAA brush both (a) before and (b) after treatment with aqueous silver acetate.

oxygen content detected in the XPS spectra may be due to the PMA block.

XPS spectra were also taken of the Si/SiO_2//PS-*b*-PAA before and after treatment with aqueous sodium tetrachloropalladate. The results were similar to those of the Si/SiO_2//PS-*b*-PAA brush before and after treatment with aqueous silver acetate. However, the XPS spectra indicated a palladium content of 6.6%. Again, it was concluded that the palladium is attached to the PAA block of the brush, as the IR spectra displayed a carboxylate anion peak. We were unable to calculate the loading of cations from the XPS spectra in this case, as the palladium $3p^3$ peak overlaps with the oxygen 1s peak and thus interferes with the calculation.

Solvent Treatment of Polyelectrolyte Diblock Copolymer Brushes. The influence of solvent on the surface properties of diblock copolymer brushes has been previously reported.[7] Each of the polyelectrolyte diblock copolymer brushes and the Si/SiO_2//PS-*b*-PAA and Si/SiO_2//PMA-*b*-PAA brushes were treated with a solvent that was a nonsolvent for the outer block but a good solvent for the tethered block. For each of the diblock copolymer brushes DMF was used to extend the brush, as DMF is a good solvent for PS, PMA, and PAA. After treatment with DMF, the diblock copolymer brushes were treated with anisole, which is a good solvent for both PS and PMA but a nonsolvent for PAA in both the nonsalt and salt states. The water contact

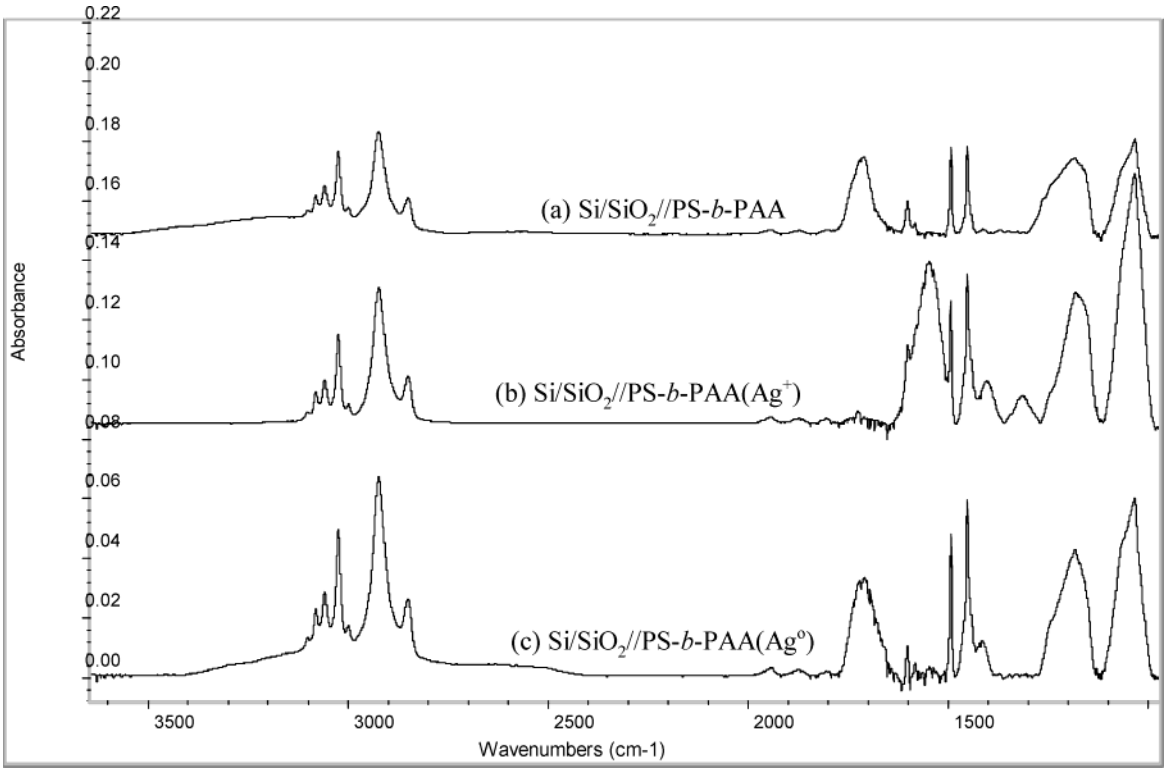

Figure 4. ATR−FTIR spectra of (a) Si/SiO_2//PS-*b*-PAA, (b) Si/SiO_2//PS-*b*-PAA(Ag^+), and (c) Si/SiO_2//PS-*b*-PAA(Ag^0).

Scheme 2. Reduction of Si/SiO_2//PS-*b*-PAA(Ag^+) to Si/SiO_2//PS-*b*-PAA(Ag°) Using H_2

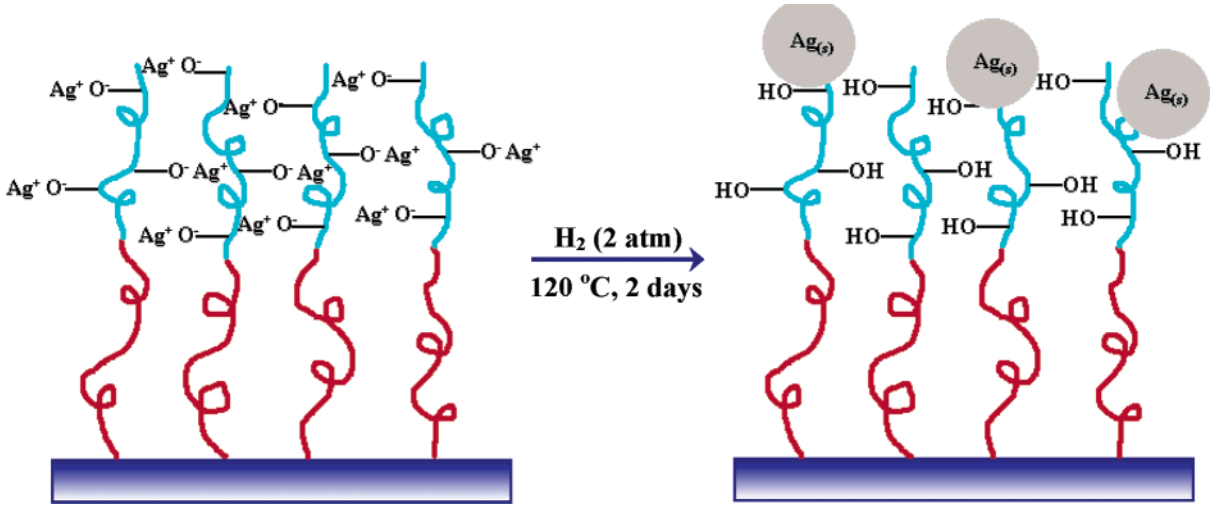

angle of the brushes was measured after each solvent treatment. In each case, after treatment with DMF the advancing contact angle of all of the samples was low (<40°) due to the presence of either PAA or the salt form of PAA at the interface. When the samples were subsequently treated with anisole, the advancing contact angles increased slightly; however, the values obtained were nowhere near the characteristic advancing contact angles of PS (≈100°) or PMA (≈76°). The maximum advancing contact angle obtained after treatment with anisole was 48°, indicating that surface rearrangement of the diblock copolymer brushes was very limited. Previous reports have indicated that surface rearrangement is strongly dependent upon the Flory−Huggins interaction parameter between the two blocks.[7] In this case, it appears as though the interaction parameter between either PS or PMA and the PAA, in either the salt or nonsalt form, is high enough to inhibit surface rearrangement of the diblock copolymer brushes.

Reduction of the Polyelectrolyte Diblock Copolymer Brushes. It has been previously reported that nanocomposites of inorganic nanoparticles embedded within polymer matrixes can be synthesized using polyelectrolyte multilayer films.[27−29] This technique relies on the synthesis of polyelectrolyte multilayer films with a controlled content of free carboxylic acid binding groups. These binding groups can then be used to bind various inorganic ions that can be subsequently reduced to nanoparticles. To date there has been no report on the use of tethered diblock copolymer brushes to produce inorganic nanoparticles. To examine the suitability of polyelectrolyte diblock copolymer brushes to produce inorganic nanoparticles, the Si/SiO_2//PS-*b*-PAA(Ag^+) and Si/SiO_2//PS-*b*-PAA(Pd^{2+}) brushes were both reduced in

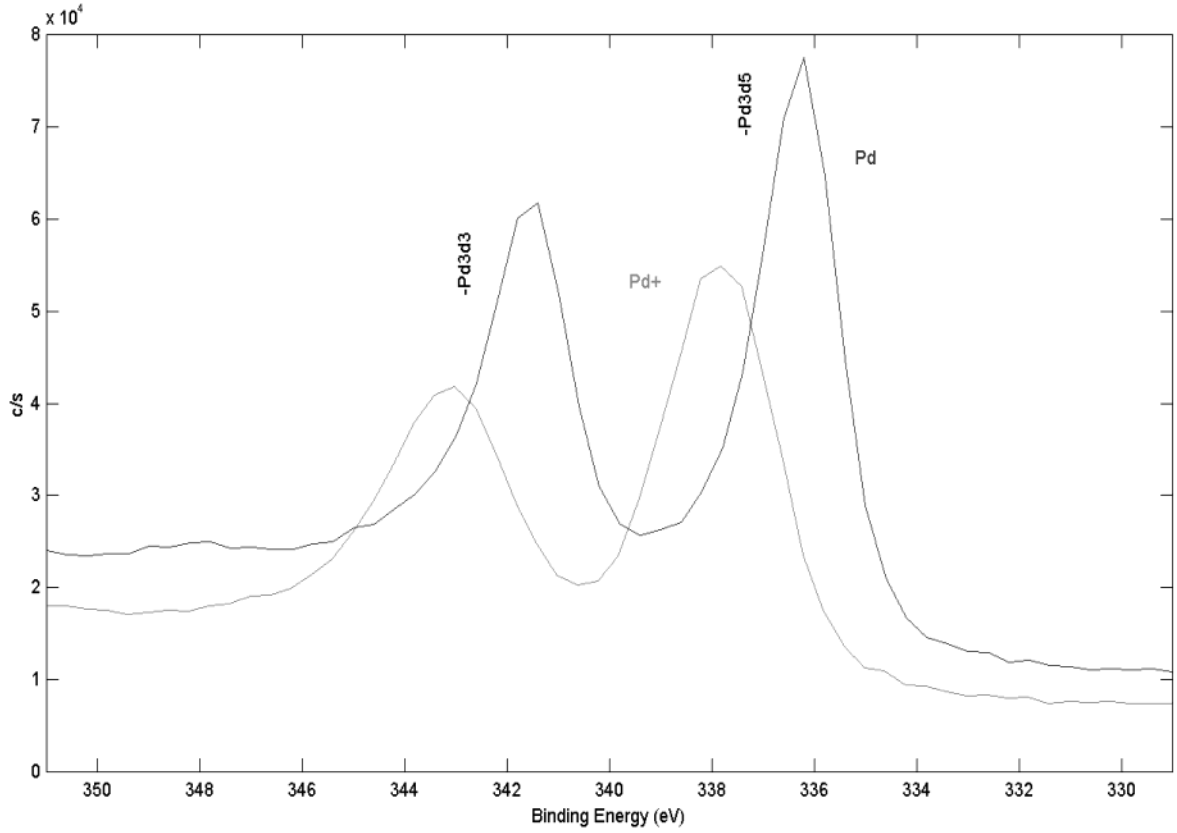

Figure 5. Expanded XPS spectra of the Pd $3d^3$ and $3d^5$ peaks for the Si/SiO_2//PS-*b*-PAA(Pd^{2+}) brush before and after reduction.

the presence of H_2 (2 atm) in an attempt to produce nanoparticles from the cationic precursors (Scheme 2).

The ATR−FTIR spectra for synthesis of the Si/SiO_2//PS-*b*-PAA(Ag^0) brush are shown in Figure 4. The formation of the Si/SiO_2//PS-*b*-PAA(Ag^+) brush from a Si/SiO_2//PS-*b*-PAA brush is evidenced by the loss of the broad OH peak at 2900−3400 cm^{-1} and the carbonyl peak at 1710 cm^{-1} and formation of the carboxylate anion peak at 1548 cm^{-1} (Figure 4a,b). After the Si/SiO_2//PS-*b*-PAA(Ag^+) brush is reduced in the presence of H_2 (2 atm) at 120 °C for 2 days, the ATR−FTIR spectra show the re-formation of the broad OH peak and the carbonyl peak at 1712 cm^{-1} and loss of the carboxylate anion peak (Figure 4c). These results indicate that after the reduction reaction the PAA block of the brush shifts from the ionized form to the protonated form, which suggests that the silver ions are potentially being reduced to zerovalent silver nanoparticles. The water contact angle and the thickness of the brush were measured before and after the reduction reaction. After reduction of the Si/SiO_2//PS-*b*-PAA(Ag^+) brush, the advancing contact angle increased from 35° to 66° while the thickness of the outer block decreased from 11 to 9 nm. The increase in contact angle is attributed to the presence of silver nanoparticles at the interface of the polymer brush, as it has been previously reported that metallic silver can have an advancing contact angle as high as 110° depending on the degree of oxidation at the metal surface and on the presence of organic impurities.[32] Similar results were also seen for the reduction of the Si/SiO_2//PS-*b*-PAA(Pd^{2+}) brush. However, in the case of the Si/SiO_2//PS-*b*-PAA(Pd^{2+}) brush, there was only a slight increase in the advancing contact angle seen after the reduction reaction, from 26° to 28°. Previous work has demonstrated that the presence of nanoparticles of palladium typically produce surface with a high degree of wettability.[33] In this work, Schulz and co-workers demonstrated that a Ti-protected silicon wafer coated with 20 nm palladium particles exhibited an advancing water contact angle of 18°.

XPS was used to confirm that the silver and palladium were still present in the diblock copolymer brushes after the reduction reaction had been performed and also to examine whether there was any difference between the peaks of the metals in their ionic and reduced forms. The main peaks in the XPS spectra of the Si/SiO_2//PS-*b*-PAA(Ag^0) brush were carbon (80.5%), oxygen (13.2%), silver (4.9%), calcium (0.5%), and trace amounts of silicon, sulfur, and chlorine. Using the same calculation as mentioned previously and the amount of oxygen present in the Si/SiO_2//PS-*b*-PAA(Ag^0) brush, the degree of loading of metal onto the PAA block was determined to be 87%. This is in very good agreement with the calculated loading of silver ions on the Si/SiO_2//PS-*b*-PAA(Ag^+) brush, which was 88%, indicating that essentially all of the silver remains within the brush after the reduction reaction. Comparison of the XPS spectra for the Si/SiO_2//PS-*b*-PAA(Ag^+) and Si/SiO_2//PS-*b*-PAA(Ag^0) brushes indicated a slight shift to lower binding energies for the silver $3d^3$ and $3d^5$ peaks in the Si/SiO_2//PS-*b*-PAA(Ag^0) brush. This result suggests that the silver detected in the Si/SiO_2//PS-*b*-PAA(Ag^0) brush is in a reduced form when compared to the silver present in the Si/SiO_2//PS-*b*-PAA(Ag^+) brush. Similar results were seen for XPS spectra of the Si/SiO_2//PS-*b*-PAA(Pd^0) brush. In this case the main peaks in the spectra were carbon (51.4%), oxygen (33.0%), palladium (7.0%), nitrogen (3.4%), silicon (1.8%), and trace amounts of

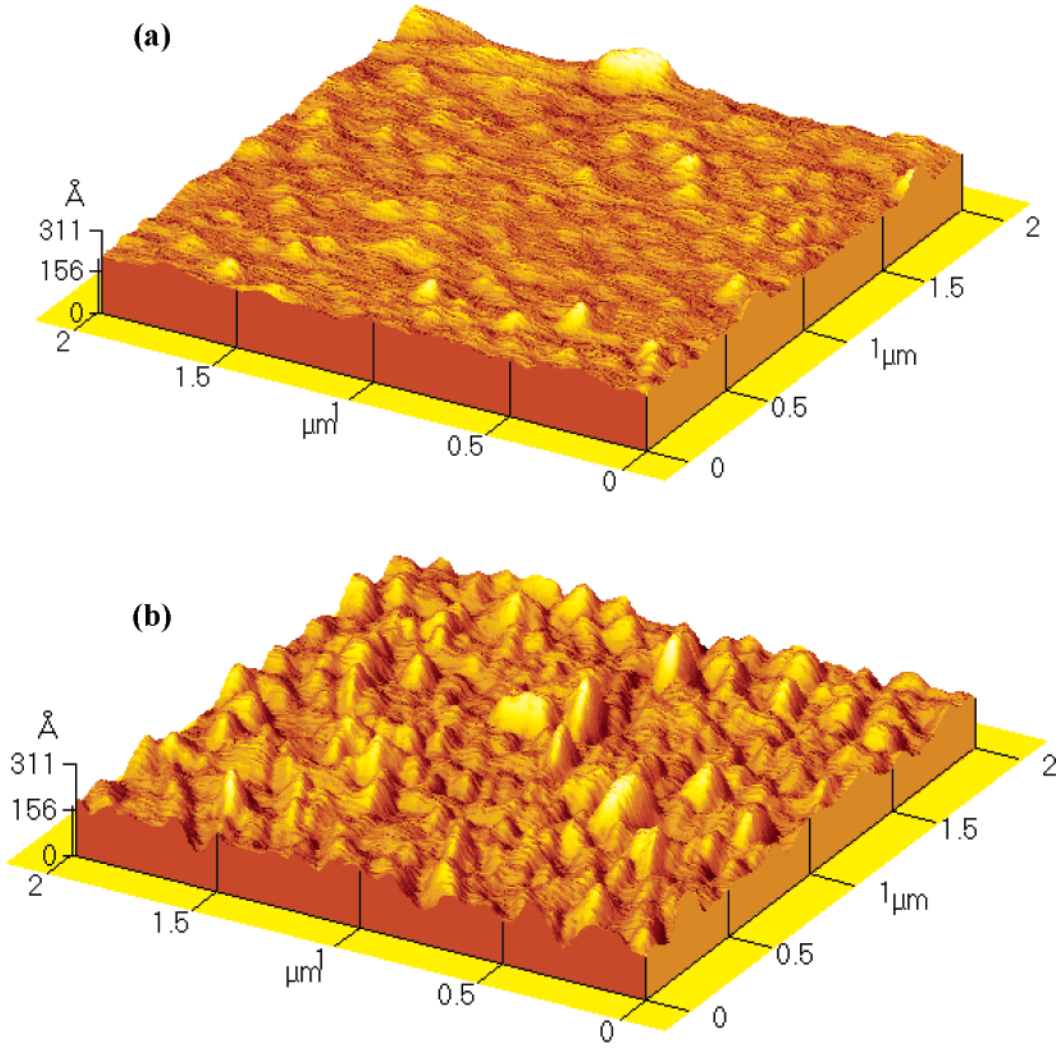

Figure 6. AFM images of (a) Si/SiO_2//PS-*b*-PAA(Ag^+) and (b) Si/SiO_2//PS-*b*-PAA(Ag^0).

sulfur, iron, sodium, and chlorine. As mention previously, loading of the palladium on to the PAA block cannot be calculated due to overlap between the palladium $3p^3$ peak and the oxygen 1s peak. However, the actual amounts of palladium present in the Si/SiO_2//PS-*b*-PAA(Pd^{2+}) and the Si/SiO_2//PS-*b*-PAA(Pd^0) brushes were in good agreement, 6.6 and 7%, respectively. Figure 5 shows a comparison between the palladium $3d^3$ and $3d^5$ peaks in the XPS spectra of the Si/SiO_2//PS-*b*-PAA(Pd^{2+}) and Si/SiO_2//PS-*b*-PAA(Pd^0) brushes. As can be clearly seen, the palladium $3d^3$ and $3d^5$ peaks for the Si/SiO_2//PS-*b*-PAA(Pd^0) brush are shifted to a lower binding energy, again suggesting that the palladium present in this sample is in a reduced form.

The intermittent-contact mode AFM images of polyelectrolyte brushes were taken both before and after reduction to monitor the changes in the topography of the surface. Figure 6 shows the AFM images of the Si/SiO_2//PS-*b*-PAA(Ag^+) and Si/SiO_2//PS-*b*-PAA(Ag^0) brushes. In Figure 6a, the AFM image of the Si/SiO_2//PS-*b*-PAA(Ag^+) shows a relatively smooth surface with occasional "bumps" and a root-mean-square (rms) roughness of 0.7 nm. After reduction of the Si/SiO_2//PS-*b*-PAA(Ag^+) brush to Si/SiO_2//PS-*b*-PAA(Ag^0) (Figure 6b), the rms roughness increased to 3 nm, and AFM image indicates the presence of defined surface features. The presence of prominent surface features and increase in rms roughness are consistent with the formation of silver nanoparticles within the diblock copolymer brush. An analysis of many randomly drawn line profiles suggests an average height for the "bumps" of 11.2 nm for the Si/SiO_2//PS-*b*-PAA(Ag^0) sample and an average height of 4.2 nm for the "bumps" in the Si/SiO_2//PS-*b*-PAA(Ag^+) brush surface. The change of average height of features between the two images is 7 nm. While supposing that the particles are 7 nm in diameter is consistent with the data available, we cannot simply assign this change to a particle diameter because we do not know how the particles are sitting in the brush. Since the top layer is soft and the surface energy of Ag^0 is high, the particles could be at least partially embedded in the brush. If the particles are spherical, which they will tend to be to minimize interfacial energy, supposing that they are at least 7 nm in diameter provides a convenient rationalization for the appearance of the larger bumps. It is possible to provide a high upper bound on the particle size. They cannot be larger than the sum of the nominal brush thickness (32 nm) and the heights of the bumps (11 nm). Because of the heights of the bumps, their apparent lateral dimensions must reflect substantial convolution with the tip dimension. That fact together with a large standard deviation in the lateral sizes of these raised features suggests that it is unwise to attempt to infer anything about the particle sizes from those lateral dimensions. Similar results were seen for the reduction of the Si/SiO_2//PS-

b-PAA(Pd^{2+}) polyelectrolyte brush. Further investigations with scanning probe microscopy are in progress to clarify the sizes of the particles.

Conclusions

Tethered diblock copolymers of either styrene or methyl acrylate and *tert*-butyl acrylate were synthesized using sequential ATRP from the self-assembled monolayer of a bromoisobutyrate initiator. Polyelectrolyte diblock copolymer brushes were subsequently formed from these samples by hydrolysis of the *tert*-butyl groups followed by treatment with aqueous metal salts. Using this technique, Si/SiO_2//PS-*b*-PAA(Ag^+), Si/SiO_2//PMA-*b*-PAA(Ag^+), and Si/SiO_2//PS-*b*-PAA(Pd^{2+}) brushes were synthesized and characterized using ATR−FTIR, goniometry, XPS, and ellipsometry. Treatment of the polyelectrolyte diblock copolymer brushes with different solvents did not result in surface rearrangement, most likely due to a high interaction parameter between the different components. The polyelectrolyte brushes were reduced using H_2 and then characterized using ATR−FTIR, tensiometry, XPS, AFM, and ellipsometry. The XPS results indicate that the metal cations are reduced during treatment with H_2, suggesting the formation of zerovalent metal within the polymer brush. AFM analysis of the brushes before and after reduction demonstrates that upon treatment with H_2 the brush surface changes from smooth and featureless to having definite surface features, which we attribute to the formation of metal nanoparticles with in the polymer brush.

Acknowledgment. This work was supported by the National Science Foundation (DMR-0072977). We thank Dr. W. Jennings for assistance with XPS.

References and Notes

(1) Milner, S. T. *Science* **1991**, *251*, 905.
(2) Halpern, A.; Tirrell, M.; Lodge, T. P. *Adv. Polym. Sci.* **1992**, *100*, 31.
(3) Zhulina, E. B.; Singh, C.; Balazs, A. C. *Macromolecules* **1996**, *29*, 6338.
(4) Zhulina, E. B.; Singh, C.; Balazs, A. C. *Macromolecules* **1996**, *29*, 8254.
(5) Ito, Y.; Nishi, S.; Park, Y. S.; Imanishi, Y. *Macromolecules* **1997**, *30*, 5856.
(6) Park, Y. S.; Ito, Y.; Imanishi, Y. *Macromolecules* **1998**, *31*, 2606.
(7) Zhao, B.; Brittain, W. J.; Zhou, W.; Cheng, S. Z. D. *Macromolecules* **2000**, *33*, 8821.
(8) Zhao, B.; Brittain, W. J.; Zhou, W.; Cheng, S. Z. D. *J. Am. Chem. Soc.* **2000**, *122*, 2407.
(9) Kong, X.; Kawai, T.; Abe, J.; Iyoda, T. *Macromolecules* **2001**, *34*, 1837.
(10) Zhao, B.; Brittain, W. J. *Prog. Polym. Sci.* **2000**, *25*, 677.
(11) Mansky, P.; Liu, Y.; Huang, E.; Russell, T. P.; Hawker, C. *Science* **1997**, *275*, 1458.
(12) Matyjaszewski, K. In *Controlled/Living Radical Polymerization*; Matyjaszewski, K., Ed.; ACS Symposium Series 768; American Chemical Society: Washington, DC, 2000; p 2.
(13) Prucker, O.; Rühe, J. *Macromolecules* **1998**, *31*, 592.
(14) Prucker, O.; Rühe, J. *Macromolecules* **1998**, *31*, 602.
(15) Husseman, M.; Malmstrom, E. E.; McNamara, M.; Mate, M.; Mecerreyes, O.; Benoit, D. G.; Hedrick, J. L.; Mansky, P.; Huang, E.; Russell, T. P.; Hawker, C. J. *Macromolecules* **1999**, *32*, 1424.
(16) Matyjaszewski, K.; Miller, P. J.; Shukla, N.; Immaraporn, B.; Gelman, A.; Luokala, B. B.; Siclovan, T. M.; Kickelbick, G.; Vallant, T.; Hoffmann, H.; Pakula, T. *Macromolecules* **1999**, *32*, 8716.
(17) Ejaz, M.; Yamamoto, S.; Ohno, K.; Tsujii, Y.; Fukuda, T. *Macromolecules* **1998**, *31*, 5934.
(18) Boyes, S. G.; Brittain, W. J.; Weng, X.; Cheng, S. Z. D. *Macromolecules* **2002**, *35*, 4960.
(19) Ejaz, M.; Ohno, K.; Tsujii, Y.; Fukuda, T. *Macromolecules* **2000**, *33*, 2870.
(20) Kong, X.; Kawai, T.; Abe, J.; Iyoda, T. *Macromolecules* **2001**, *34*, 1837.
(21) Osborne, V. L.; Jones, D. M.; Huck, W. T. S. *Chem. Commun.* **2002**, 1838.
(22) Seidel, C. *Macromolecules* **2003**, *36*, 2536.
(23) Mercurieva, A. A.; Birshtein, T. M.; Zhulina, E. B.; Iakovlev, P.; van Male, J.; Leermakers, F. A. M. *Macromolecules* **2002**, *35*, 4739.
(24) Zhulina, E. B.; Klein Wolterink, J.; Borisov, O. V. *Macromolecules* **2000**, *33*, 4945.
(25) Habicht, J.; Schmidt, M.; Rühe, J.; Johansmann, D. *Langmuir* **1999**, *15*, 2460.
(26) Balastre, M.; Li, F.; Schorr, P.; Yang, J.; Mays, J. W.; Tirrell, M. V. *Macromolecules* **2002**, *35*, 9480.
(27) Clay, R. T.; Cohen, R. E. *Supramol. Sci.* **1995**, *2*, 183.
(28) Joly, S.; Kane, R.; Radzilowski, L.; Wang, T.; Wu, A.; Cohen, R. E.; Thomas, E. L.; Rubner, M. F. *Langmuir* **2000**, *16*, 1354.
(29) Wang, T. C.; Rubner, M. F.; Cohen, R. E. *Langmuir* **2002**, *18*, 3370.
(30) Keller, R. N.; Wycoff, H. D. *Inorg. Synth.* **1946**, *2*, 1.
(31) Zhao, B.; Brittain, W. J. *Macromolecules* **2000**, *33*, 8813.
(32) Osman, M. A.; Keller, B. A. *Appl. Surf. Sci.* **1996**, *99*, 261.
(33) Schulz, F.; Franzka, S.; Schmid, G. *Adv. Funct. Mater.* **2002**, *12*, 532.

MA035029C